Proceedings of the 28th IEEE
EMBS Annual International Conference
New York City, USA, Aug 30-Sept 3, 2006

Automated 3D Elastic Registration for Improving Tumor Localization in Whole-body PET-CT from Combined Scanner

Vivek Walimbe, *Student Member, IEEE*, Omkar Dandekar, *Student Member, IEEE*, Faaiza Mahmoud, Raj Shekhar*, *Member, IEEE*

***Abstract*—Combined PET/CT scanners provide the ability to produce matching metabolic (from PET) and anatomic (from CT) information in a single examination. However, misalignments continue to exist in tumor localization in PET and CT images acquired using these scanners, due to their inability to compensate for nonrigid misalignment resulting from patient breathing and involuntary movement. We demonstrate that our automatic image subdivision-based elastic registration algorithm can correct this misalignment. In a quantitative validation involving 13 expert-identified tumor nodules in six PET-CT image pairs, the algorithm demonstrated statistically significant improvement over the scanner-defined localization. The accuracy of algorithm-determined localization was evaluated to be comparable to average manually defined localization. The results indicate the potential of using our registration algorithm for applications like radiotherapy treatment planning and treatment-monitoring involving combined PET/CT scanners**

I. Introduction

Multimodality registration of images acquired by whole-body computed tomography (CT) and positron emission tomography (PET) provides simultaneous access to complementary anatomic and physiologic information, respectively, from the two images. Fusion of the registered multimodality images enables accurate localization of viable tumors visible in PET with respect to the anatomical information from CT for assessment of disease progression, treatment planning, and surgical interventions [1]. We have previously reported an image subdivision-based method for automatic elastic registration of whole-body CT and PET images from separate as well as combined scanners [3], and the registration accuracy was validated to be on par with the average opinion of three experts. We also demonstrated that the software-based registration algorithm improves upon the mechanical registration of combined PET/CT scanners by eliminating any nonrigid residual misalignment due to breathing-related or patient motion artifacts [3]. For cancerous nodules in the lung, studies have reported that breathing- and patient motion-related artifacts introduce a misalignment of the order of 7-8 mm between PET and CT acquired using the combined scanners [1]. In the current work we focus on evaluation of the accuracy of our registration algorithm to localize viable tumors in PET with respect to the anatomy in CT, for images acquired using a combined PET/CT scanner.

V. Walimbe is with the Biomedical Engineering Dept., The Ohio State University, Columbus, OH 43210, USA and Dept. of Biomedical Engineering, Lerner Research Institute, The Cleveland Clinic, Cleveland, OH 44195, USA (e-mail: walimbe.2@osu.edu).

O. Dandekar is with the Dept. of Diagnostic Radiology, University of Maryland, Baltimore, MD 21201, USA and Dept. of Electrical & Computer Engineering, University of Maryland, College Park, MD 20740, USA (email: dandekar@ieee.org).

F.Mahmoud is with the VA Maryland Health Care System, Baltimore, MD 21201, USA (email: faaiza@siddiqui.md).

*R. Shekhar is with the Dept. of Diagnostic Radiology, University of Maryland, Baltimore, MD 21201, USA (phone: 410-706-8714; fax: 410-706-8724; e-mail: rshekhar@umm.edu).

II. Registration Algorithm

We present here a brief overview of our elastic registration algorithm that has previously been described in detail in [3, 4].

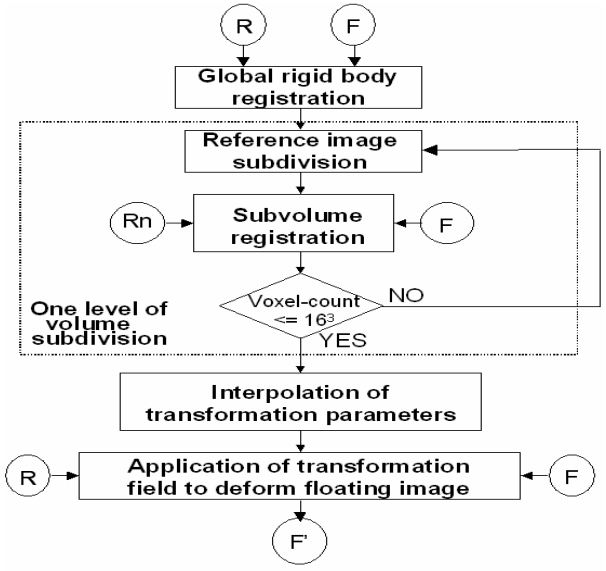

Fig. 1. Flowchart of registration algorithm. R: reference image, F: floating image, Rn: subvolumes of reference image, and F′: transformed floating image, after registration with reference image

For a pair of reference and floating images, our registration algorithm initially recovers the global mismatch, followed by hierarchical refinement of the localized matching between the globally registered images. Global registration uses the six-parameter rigid-body transformation model and is based on maximization of normalized mutual information (NMI) between the two images. Next, we implement a hierarchical octree-based subdivision scheme. At each subdivision level, the floating image is registered

with the individual subvolumes of the reference image, considered one at a time. Volume subdivision and subvolume registration continue until the voxel count for an individual subvolume remains above a predefined limit. Subvolume registration also uses a six-parameter rigid-body transformation model. Initial seeding of the undivided floating image with respect to each subvolume is given by the transformation obtained from registration involving the floating image and the corresponding parent subvolume at the previous level of subdivision. Subvolume registration is based on maximization of NMI, and uses the prior registration information for all remaining parts of the image, available from the previous hierarchical level. Subvolume registration is constrained by the maximum allowable deformation, in order to maintain image integrity by preventing individual subvolumes from drifting far off from their starting positions at each hierarchical level.

After registration at the last hierarchical level, the transformations are assigned to centers of the respective subvolumes. A unique transformation is determined for every voxel in the reference image by performing tri-cubic interpolation between the subvolume centers surrounding the voxel. The 3D translational component of the transformation is interpolated separately as three scalars. Interpolation of 3D rotation is performed in the quaternion domain, by converting the rotational matrices into quaternions. Use of the six-parameter rigid-body transformation model for subvolume registration and direct interpolation of the subvolume transformations for generation of smooth transformation field are unique features of our registration algorithm. Using the transformation field, each grid point from the reference image space is mapped to find the matching location in the floating image space. The intensity at this location in floating image space is determined using a trilinear interpolation scheme and assigned to the original grid point in the reference image space, resulting in a continuous elastically transformed floating image.

III. Materials and Methods

We registered six pairs of whole-body PET-CT images, acquired in clinical settings using a combined PET/CT scanner (Philips Gemini PET/CT 16). The six image pairs were selected by a clinical expert, not conversant with the working of the registration algorithm, based on the presence of single/multiple malignant tumors visible in both PET and CT. CT images were 512 × 512 × 187-243 voxels with voxel dimensions 1.17 mm × 1.17 mm × 4 mm. The typical PET image size varied between 150 × 150 × 187-243 voxels, with cubic voxels of dimensions 4 mm × 4 mm × 4 mm. During CT and PET image acquisition, subjects were instructed to keep arms beside the body and perform shallow breathing. 18F-FDG was injected as radiotracer. Low dose non contrast-enhanced CT image was acquired first, immediately followed by the PET image acquisition. No transmission PET scan was acquired, and the attenuation correction for PET was performed using the CT image. CT was used as the reference image and PET was deformed following the registration to match the reference CT image. The registration process was fully automatic, with no manual intervention steps.

A physician, experienced in interpreting whole-body PET and CT images, identified a total of 13 tumors in the six cases. These expert-identified tumors were manually segmented in PET and CT by three observers blinded to the identities of the subjects. Each expert-identified tumor was outlined in predefined axial slices in both PET and CT images independently by the three observers. The centroid calculated for each set of observer-drawn contours in an image is the best single-point representation of corresponding tumor localization by that expert in the given image, and this representation was used for comparing the manual, algorithm-defined and scanner-determined tumor localizations.

We calculated CT_1, CT_2, and CT_3 as the sets of centroid locations for all tumors as identified by the three observers in CT, and PET_1, PET_2, and PET_3 as sets of centroid locations in PET. A "test centroid location" was created for each tumor in CT by averaging the centroid locations as determined by the three observers (CT_{TEST} = Average$\{CT_1,CT_2,CT_3\}$). The algorithm-determined transformation field corresponding to each image-pair was then used to determine a set of tumor locations in the PET image (PET_{ALGO}) representing the transformed locations of the corresponding points in CT_{TEST} after the automatic elastic registration. The four sets of PET points - PET_1, PET_2, PET_3, and PET_{ALGO} – were allocated to four separate groups of three sets each ($^4C_3$). Group 1: PET_1, PET_2, PET_3; Group 2: PET_1, PET_2, PET_{ALGO}; Group 3: PET_1, PET_3, PET_{ALGO}; and Group 4: PET2, PET_3, PET_{ALGO}. For each group, the mean difference in the transformed location of corresponding tumor centroids was obtained for all pair-wise combinations of sets of PET points within that group. Good agreement between the algorithm-determined centroid locations and the three manually determined localizations is indicated by comparable values of mean difference obtained for all four groups. Significantly increased (or decreased) values of the mean difference for Group 2, Group 3 or Group 4 compared with Group 1 would indicate that the three sets of PET points in that group show less (or more) interobserver variability compared with the three sets in Group 1. Similar analysis was performed by replacing the algorithm-determined locations of centroids in PET with the scanner-determined locations ($PET_{SCANNER}$), to evaluate the level of agreement between the manually determined and scanner-determined locations of tumor centroid locations.

Williams' Index (WI), a statistical measure of interobserver variability, was calculated for the four groups, first including the algorithm-determined and then the scanner-defined centroid locations. WI provides a metric to

evaluate the performance of the computer algorithm-determined (or scanner-defined) tumor localization in context of the variability in manually defined localization. A value of WI close to 1.0 indicates that the algorithm-determined (or scanner-defined) localization agrees with the manual localizations as much as the manually defined localizations agree among themselves.

IV. Results

Registration was performed on a Dell workstation (Xeon 2.00-GHz processor, 2.00-GB RAM) running Microsoft Windows® XP Professional. The average execution time for registration of a single dataset was approximately 50 min. All the six image pairs showed improvement in image matching post-registration. See typical example in Figure 2.

Table I shows the comparison of the algorithm-determined (and scanner-defined) localization of tumors with respect to the average manually determined localization, using the mean difference in transformed locations of tumor-centroids calculated for Groups 1-4. In Table I, when analyzing the algorithm-determined localization, the mean value for any given group lies within the 95% confidence interval (CI) of the mean for the remaining three groups, which indicates that the performance of the registration algorithm for tumor localization is comparable to the average observer performance. A statistically significant ($p < 0.05$) larger mean difference value, whenever the scanner-defined localization was included in a group, indicates that the performance of the combined PET/CT scanner was slightly inferior compared with the average observer performance. Elastic registration using our algorithm improved accuracy of tumor localization, which is evident from improved (smaller) mean difference values for Groups 2-4 in Table I when our algorithm-determined registration was used in place of scanner-defined registration for tumor localization.

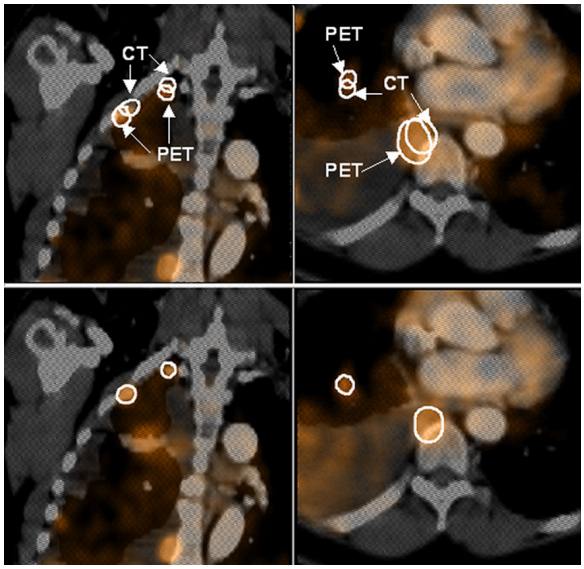

Fig. 2. Misalignment in tumor localization in PET/CT images from combined scanner. Top row shows two cross-sectional views of fused PET/CT illustrating the misalignment for four different tumors. Contours indicate the misaligned tumor locations in PET and CT. Bottom row shows the results after software registration. Contours indicate the registered tumor locations in the fused image.

TABLE I
GROUPWISE COMPARISON OF VARIABILIY IN TUMOR LOCALIZATION
P1: PET_1, P2: PET_2, P3: PET_3

PX	Difference in landmark location – mean (mm) and 95% confidence interval - CI (mm)			
	Group 1 P1,P2, P3	**Group 2** P1,P2, PX	**Group 3** P1,P3, PX	**Group 4** P2,P3, PX
PET_{ALGO}	4.2	4.4	4.5	4.6
	3.5 - 4.9	3.5 - 5.3	3.6 - 5.4	3.6 - 5.6
$PET_{SCANNER}$	4.2	5.8	6.0	5.6
	3.5 - 4.9	5.0 - 6.7	5.3 - 6.7	4.8 - 6.4

P1: PET_1, P2: PET_2, P3: PET_3

For algorithm-determined localization, the 95% CI for WI includes the value 1.0 (Table II), indicating that the performance of the automatic elastic registration algorithm is within the limits of interobserver variability in manually defined localization. A lower value of WI (Table II) when scanner-defined registration is used in place of algorithm-defined registration indicates that the variability is higher between the scanner-defined and average manually defined localization than between algorithm-defined and average manually defined localization.

V. Discussion

Accurate anatomic localization of functional abnormalities seen on PET scans is known to be challenging due to the lack of detailed, high-resolution anatomy. The emergence of combined PET/CT scanners in the recent years has provided a potential solution to this issue through the ability to produce a study combining metabolic (from PET) and anatomic (from CT) information in a single examination. In patients with suspected cancerous lesions, the "anatomo-metabolic" information from PET/CT images has been reported to increase the number of definite localizations by 41% in the thorax and 66% in the abdomen, and has been reported to reduce the number of probable and equivocal lesions by 32% in thorax and 50% in abdomen [1].

The direct fusion of metabolic PET and high-resolution anatomical CT images acquired using the combined scanner

TABLE II
WILLIAMS' INDEX VALUES FOR VARIABILITY IN LANDMARK IDENTIFICATION

	Williams' Index (WI)	**95% confidence interval (CI)**
Algorithm	0.97	0.91 – 1.04
Scanner	0.89	0.81 – 0.97

is based on the assumption that the two images are accurately registered spatially. The combined PET/CT scanners perform image registration "mechanically", by performing the two scans successively while minimizing patient movement through the use of a common couch, and then appropriately translating one scan with respect to another. Thus, these scanners, due to their very design, may neutralize any rigid misalignment, but certainly cannot compensate for nonrigid misalignment from involuntary motion of internal organs in the thorax and the abdomen. Such differences mainly arise due to involuntary patient motion during the image acquisition (complete acquisition time for PET and CT is about 40-45 min) and due to the varying breathing protocols. Whereas short scan times permit performing CT with breath-hold, longer PET scans are performed with the subject engaged in tidal breathing. Image misalignment artifacts due to respiratory motion are found in large number of cases and are pronounced in the area of the diaphragm, leading to target registration error as high as 11 mm [2]. For cancerous nodules in the lung, studies have reported a misalignment of the order of 7.6 mm between PET and CT acquired using the combined scanners [1]. Thus, there is a specific need for software-based registration algorithms to correct for such existing misalignments.

We have previously reported an automated elastic registration algorithm to correct for nonrigid misalignments in whole-body PET-CT images from combined scanners, with average registration error of 6.6 ± 3.4 mm [3]. However, due to the sparse distribution of landmarks and the lack of specific landmarks near tumor, it was not possible to exactly evaluate the accuracy of specific tumor localization based solely on the results reported in [3]. In the current work we have focused on evaluation of registration accuracy for cancerous lesions as seen in PET and CT acquired using the combined scanner, based on manually segmented tumors in six PET-CT image pairs. The results in Table II demonstrate that, in comparison to average manual localization, inaccuracies exist in tumor localizations based on the scanner-defined mechanical registration. The results in Tables I & II further indicate that localization of tumors based on our algorithm-determined nonrigid registration between PET and CT corrects for these misalignments, and improves on the localization based on the scanner registration. The corrected registration/localization is on par with the average manually defined registration. The accuracy of localization of tumors, as reported in Table I, is of the order of voxel dimensions in PET, and compares favorably to the overall registration accuracy of 6.6 ± 3.4 mm as reported in [3]. The registration process is computationally efficient; the average execution time of 50 min is on par with the time we reported previously, and compares favorably with other approaches [3].

VI. Conclusion

We have demonstrated that misalignments can exist in tumor localization in PET and CT images acquired using combined scanners, and that these can be corrected by our automatic image-subdivision-based elastic registration algorithm. The accuracy of the localization using our algorithm-determined registration was comparable to average manually-defined localization of tumors. The results indicate the potential of using our registration algorithm for applications like radiotherapy treatment planning and treatment monitoring involving combined PET/CT scanners.

Acknowledgment

The authors acknowledge Vladimir Zagrodsky, PhD (The Cleveland Clinic) and Peng Lei, MS (University of Maryland) for their help in manual segmentation of tumors in PET and CT.

References

[1] C. Cohade, R. L. Wahl, "Applications of positron emission tomography/computed tomography image fusion in clinical positron emission tomography-clinical use, interpretation methods, diagnostic improvements," *S Nucl Med*, 33; pp. 228-237, 2003.

[2] G.W. Goerres, E. Kamel, B. Seifert, et al., "Accuracy of image coregistration of pulmonary lesions in patients with non-small cell lung cancer using an integrated PET/CT system," *J Nucl Med*., 43; pp.1469-1475, 2002.

[3] R. Shekhar, V. Walimbe, S. Raja, et al., "Automated Three-Dimensional Elastic Registration of Whole-Body PET and CT from Separate or Combined Scanners," *J Nucl Med*, 46(9); pp.1488-96, 2005.

[4] V. Walimbe and R. Shekhar, "Automatic elastic image registration by interpolation of 3D rotations and translations from discrete rigid-body transformations," *Med Imag Anal*, (accepted for publication).